Measurement of jet shapes in top pair events at $\sqrt{s} = 7$ TeV using the ATLAS detector at the LHC

Javier Llorente

On behalf of the ATLAS Collaboration

DIS 2013, Marseille. 22-26 April 2013

Motivation

- This measurement aims to study the differences between *b*- and light-quarks in terms of jet shapes.
- Sensitive observables for the modelling of the parton shower.

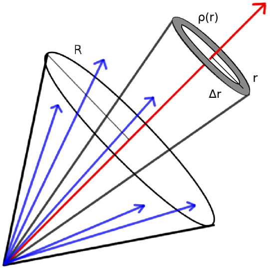

- Differential jet shape $r \leq R - \Delta r/2$

$$\rho(r) = \frac{1}{\Delta r} \frac{p_T(r - \Delta r/2, r + \Delta r/2)}{p_T(0, R)}$$

- Integrated jet shape $r \leq R$

$$\Psi(r) = \frac{p_T(0, r)}{p_T(0, R)}$$

Previous *b*-jet results by CDF [Phys. Rev. D 78, 072005 (2008)]
Inclusive jet results by ATLAS [Phys. Rev. D 83, 052003 (2011)]

Top quark production at ATLAS

- LHC: Top factory $\sigma_{t\bar{t}} = 173^{+25}_{-24}$ pb [Phys. Lett. B 711 244-263 (2012)]
- Top quark decays $t \to Wb$ are a rich and clean source of b-quarks.
- The hadronic $W \to q\bar{q}'$ decays are a source of u, d, c, s-quarks.
- Analysis with $\int Ldt = 1.8\ \mathrm{fb}^{-1}$ of 2011 data.

Single-lepton channel

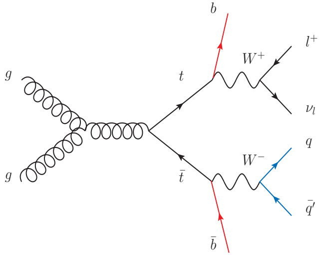

Dilepton channel

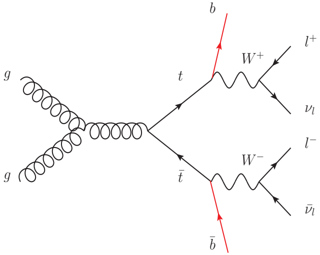

The ATLAS detector

- Multi-purpose particle detector at the LHC
- Sampling calorimeters with high granularity (3 EM layers, 3 Had layers)
- High-efficiency jet reconstruction

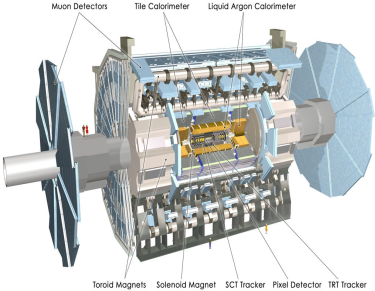

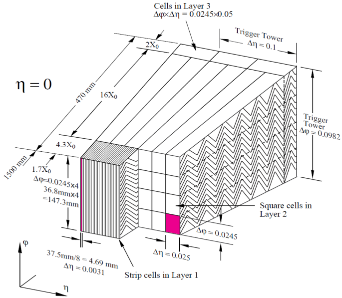

Inputs to jet reconstruction: 3-Dimensional Topological Clusters.

- Iteratively constructed from calorimeter cells.
- Seeded from $|E| > 4\sigma$ cells. $|E| > 2\sigma$ cells and perimeter cells are added.
- Variable size.
- Aim to contain the shower from each hadron.

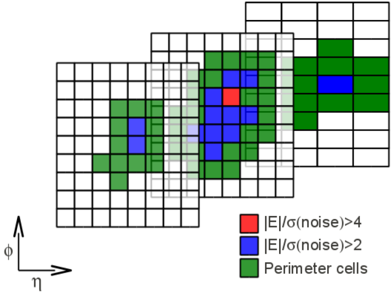

Jet algorithm: anti-k_T.

- Iterative algorithm based on the metric d_{ij}
- Infrared and collinear safe.
- Radius parameter $R = 0.4$.

$$\left.\begin{aligned} d_{ij} &= \min\left(\frac{1}{k_{Ti}^2}, \frac{1}{k_{Tj}^2}\right)\frac{\Delta R_{ij}^2}{R^2} \\ d_{iB} &= \frac{1}{k_{Ti}^2} \end{aligned}\right\}$$

Event selection (Single-lepton channel)

- Trigger: Inclusive 20 GeV electron or 18 GeV muon.
- One isolated lepton with $E_T^e > 25$ GeV or $p_T^\mu > 20$ GeV.
- At least 4 jets with $p_T > 25$ GeV and $|\eta| < 2.5$.
- At least one b-tagged jet (efficiency $\epsilon_b = 57\%$).
- $E_T^{miss} > 35$ GeV (e-channel) or $E_T^{miss} > 20$ GeV (μ-channel)
- $m_T^W > 25$ GeV (e-channel) or $m_T^W + E_T^{miss} > 60$ GeV (μ-channel).

$$m_T^W = \sqrt{2 p_T^\ell E_T^{miss} (1 - \cos \Delta\phi_{\ell\nu})}$$

Process	Expected events	Fraction
$t\bar{t}$	14000 ± 700	77.4%
W + jets ($W \to \ell\nu$)	2310 ± 280	12.8%
Other EW (Z, diboson)	198 ± 18	1.1%
Single top	668 ± 14	3.7%
Multi-jet	900 ± 450	5.0%
Total Expected	18000 ± 900	
Total Observed	17019	

Event selection (Dileptonic channel)

- Two isolated leptons with $E_T^e > 25$ GeV or $p_T^\mu > 20$ GeV.
- At least two jets with $p_T > 25$ GeV and $|\eta| < 2.5$.
- Missing energy $E_T^{miss} > 60$ GeV (ee,$\mu\mu$) and $H_T > 130$ GeV ($e\mu$).
- Dilepton invariant mass $m_{\ell\ell} > 15$ GeV and $|m_{\ell\ell} - m_Z| \geq 10$ GeV.
- At least one b-tagged jet ($\epsilon_b = 57\%$).

Process	Expected events	Fraction
$t\bar{t}$	2100 ± 110	94.9%
Z + jets ($Z \to \ell^+\ell^-$)	14 ± 1	0.6%
Other EW (W, diboson)	4 ± 2	0.2%
Single top	95 ± 2	4.3%
Multi-jet	0^{+2}_{-0}	0.0%
Total Expected	2210 ± 110	
Total Observed	2067	

To select our b and light-jet samples, the following cuts are applied

b-quark jets

- b-tagged with $\epsilon_b = 57\%$.
- $\Delta R_{bj} > 0.8$ (isolated jets).
- $|JVF| > 0.75$ to avoid pileup jets.
- Purity ($\ell q\bar{q}'$): $p_b = (88.5 \pm 5.7)\%$
- Purity ($\ell\ell$): $p_b = (99.3^{+0.7}_{-6.5})\%$

Light-quark jets u, d, c, s

- Pair with closest mass to m_W.
- Anti b-tagged with $\epsilon_b = 57\%$.
- $\Delta R_{lj} > 0.8$ (isolated jets).
- $|JVF| > 0.75$ to avoid pileup jets.
- Purity ($\ell q\bar{q}'$): $p_l = (66.2 \pm 4.1)\%$

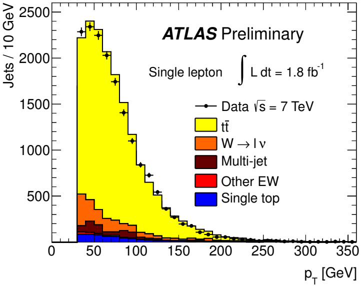

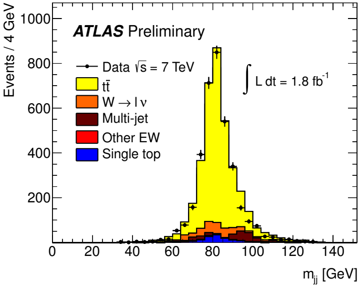

Differential jet shapes $\rho(r)$. Detector level

The left figure shows the $\rho(r)$ distributions for b-jets in the single-lepton channel. On the right, the average values $\langle\rho(r)\rangle$ for both b- and light-jets.

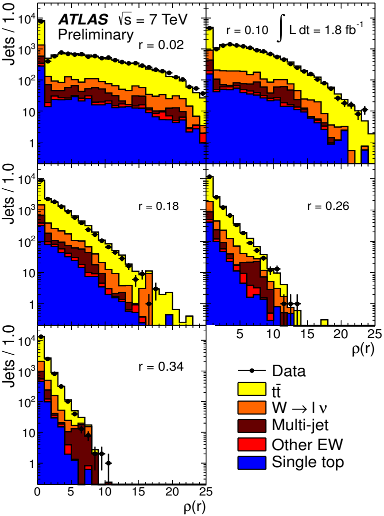

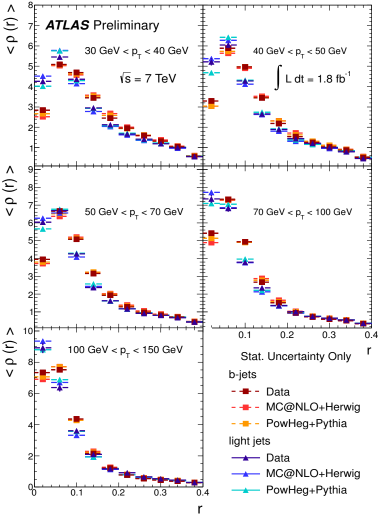

Integrated jet shapes $\Psi(r)$. Detector level

The left figure shows the $\Psi(r)$ distributions for b-jets in the single-lepton channel. On the right, the average values $\langle\Psi(r)\rangle$ for both b- and light-jets.

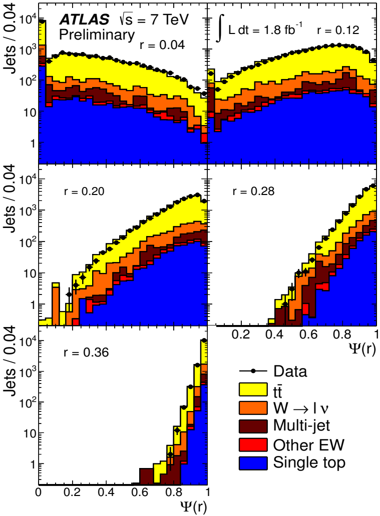

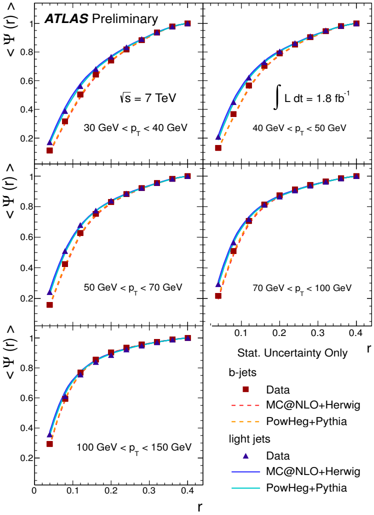

Jet shapes are found to be very dependent with jet transverse momentum p_T and mildly dependent on pseudorapidity.

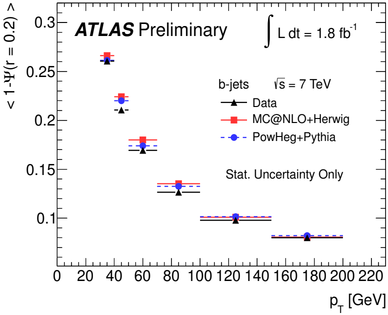

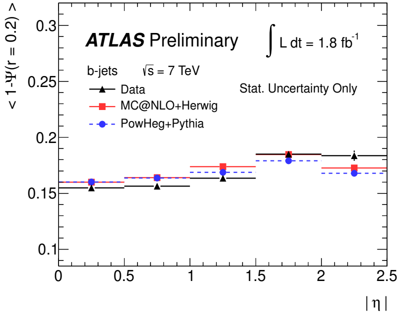

Particle jet defintion

All particle jets fulfill the same kinematic requirements than reconstructed jets: $p_T > 25$ GeV, $|\eta| < 2.5$ and $\Delta R_{jj} > 0.8$.

- Particle jets: anti-k_T jets for particles with average lifetime $\tau > 10^{-11}$ s, excluding muons and neutrinos.
- Particle b-jet: A particle jet containing a B-hadron closer than $\Delta R_{Bj} = 0.3$ to the jet axis.
- Particle light-jets: Pair of non-b particle jets with closest invariant mass to m_W.

Correction factors

Bin-by-bin factors are calculated for the average values $\langle\rho(r)\rangle$ and $\langle\Psi(r)\rangle$.

$$F^{\rho}_{l,b}(r) = \frac{\langle\rho(r)_{l,b}\rangle_{\mathrm{MC,part}}}{\langle\rho(r)_{l,b}\rangle_{\mathrm{MC,det}}}; \qquad F^{\Psi}_{l,b}(r) = \frac{\langle\Psi(r)_{l,b}\rangle_{\mathrm{MC,part}}}{\langle\Psi(r)_{l,b}\rangle_{\mathrm{MC,det}}}$$

Systematic uncertainties

For each bin (p_T, r) the total uncertainty is calculated as

$$\Delta\rho = \sqrt{(\Delta_{stat}\rho)^2 + \sum_{i=1}^{n} (\Delta_i\rho)^2}$$

Source i	Description	Impact $\Delta_i\rho/\rho$
Cluster Systematics	Energy Scale, Angular Resolution	$2\% - 10\%$
Pileup	Number of primary vertices	$2\% - 10\%$
Unfolding-Model	Parton shower modelling	$1\% - 8\%$
Jet Energy Scale	Uncertainty on the jet calibration	$\simeq 5\%$
Jet Energy Resolution	Calorimeter energy resolution σ	$\simeq 5\%$
JVF	JVF-related uncertainty	$< 1\%$

Unfolded results: 30 GeV $< p_T <$ 40 GeV

Differential $\langle \rho(r) \rangle$

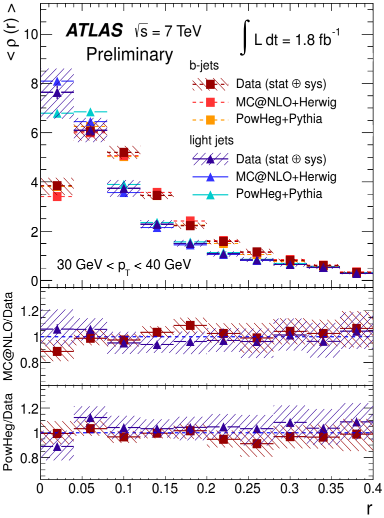

Integrated $\langle \Psi(r) \rangle$

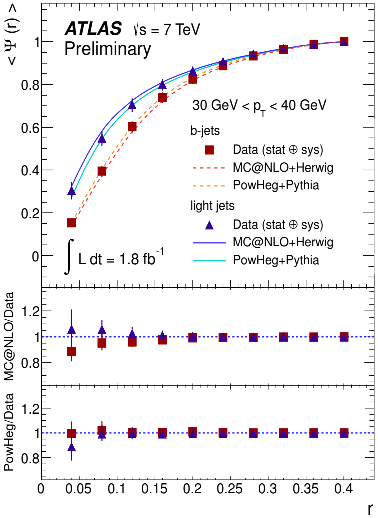

Unfolded results: 100 GeV $< p_T <$ 150 GeV

Differential $\langle\rho(r)\rangle$

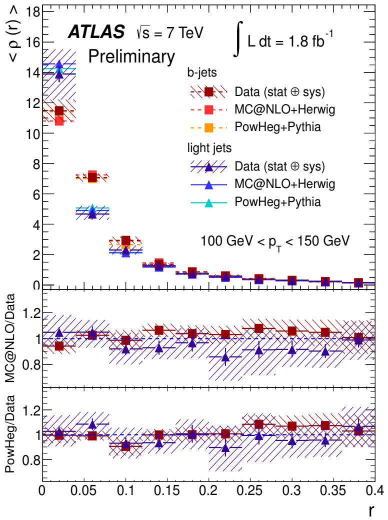

Integrated $\langle\Psi(r)\rangle$

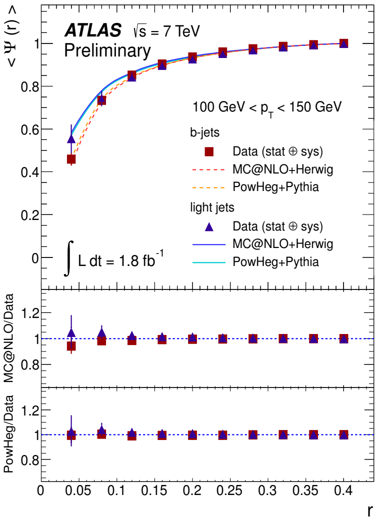

Conclusions

- We have gained insight into the jet structure of $t\bar{t}$ final states by measuring jet shapes for b (light) jets coming from top (resp. W) decays.
- They are strongly (mildly) dependent on the jet transverse momentum (resp. pseudorapidity)
- Light-jets are narrower than b-quark induced ones. The effect is visible in all p_T bins.
- Both light- and b-jets are fairly well described by MC with matrix elements up to NLO matched to parton showers, with fragmentation implemented either with Pythia or Herwig + Jimmy.

Backup Slides

Unfolded results: 40 GeV $< p_T <$ 50 GeV

Differential $\langle \rho(r) \rangle$

Integrated $\langle \Psi(r) \rangle$

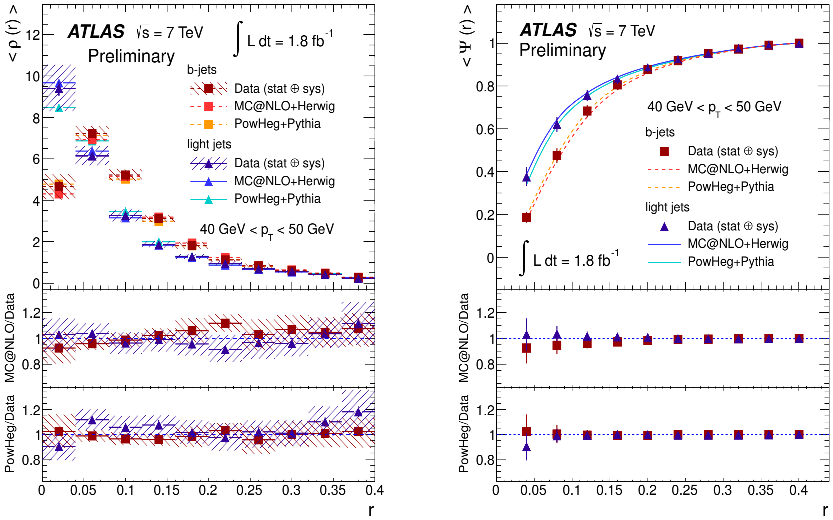

Unfolded results: 50 GeV $< p_T <$ 70 GeV

Differential $\langle \rho(r) \rangle$

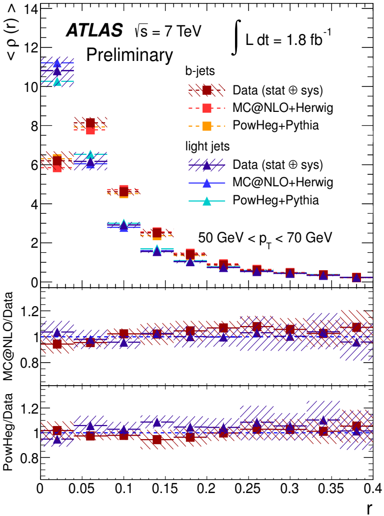

Integrated $\langle \Psi(r) \rangle$

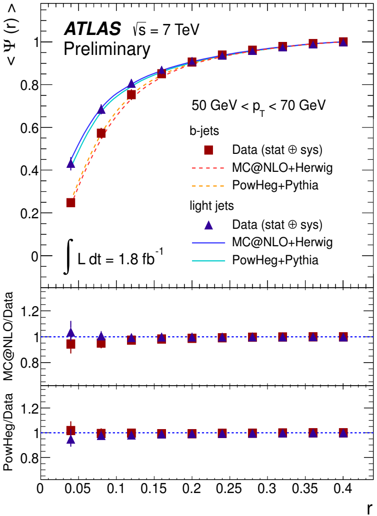

Unfolded results: 70 GeV $< p_T <$ 100 GeV

Differential $\langle \rho(r) \rangle$

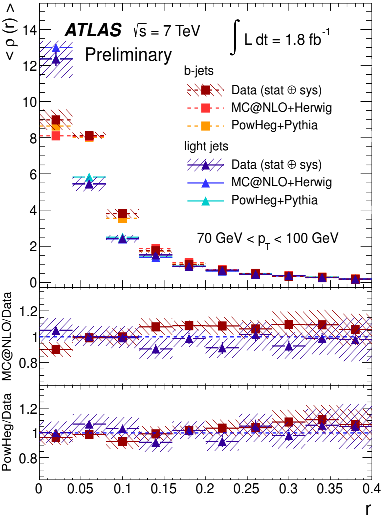

Integrated $\langle \Psi(r) \rangle$

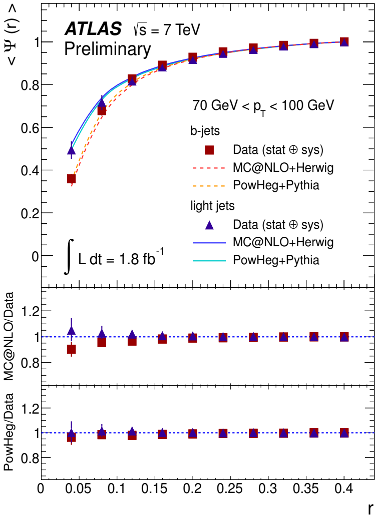

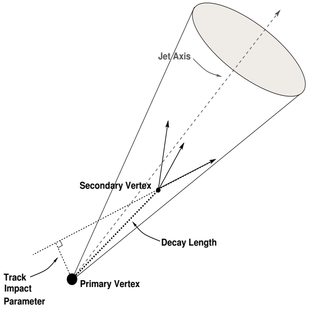

Main features

- Secondary vertex displacement.
- Impact parameter significance d_0/σ_{d_0}
- Other: Vertex mass, Energy fraction...
- Use of NN algorithms to achieve better performance.

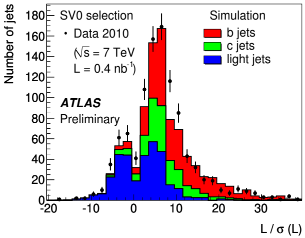

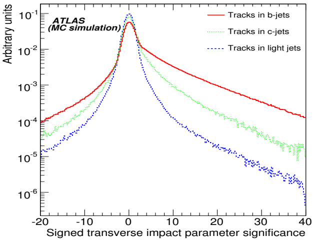

The JVF algorithm

- Variable defined for each jet and vertex (i, j).
- Fraction of p_T of tracks in the jet i associated with the vertex j
- When defined with respect to the primary interaction vertex, it provides rejection power against pileup jets. ($|JVF| > 0.75$)

$$\mathrm{JVF}(\mathrm{jet_i}, \mathrm{vtx_j}) = \frac{\sum_k p_T(\mathrm{trk_k^{jet_i}}, \mathrm{vtx_j})}{\sum_n \sum_l p_T(\mathrm{trk_l^{jet_i}}, \mathrm{vtx_n})}$$

Background estimation

Multi-jet background estimation using jet-electron method [Phys. Lett. B **717**, 330 (2012)]

- Fake lepton selection from high EM-fraction jets (jet-electron).
- Shape of the distributions estimated accordingly.
- Normalisation derived using binned-likelihood fit to the E_T^{miss} distribution.
- Same method used for muons.

All other backgrounds (W/Z+jets, Single top, ...) estimated using MC simulation.

Differential jet shapes $\rho(r)$: Comparison

The distributions for $\rho(r)$ for b (left) and light-jets (right).

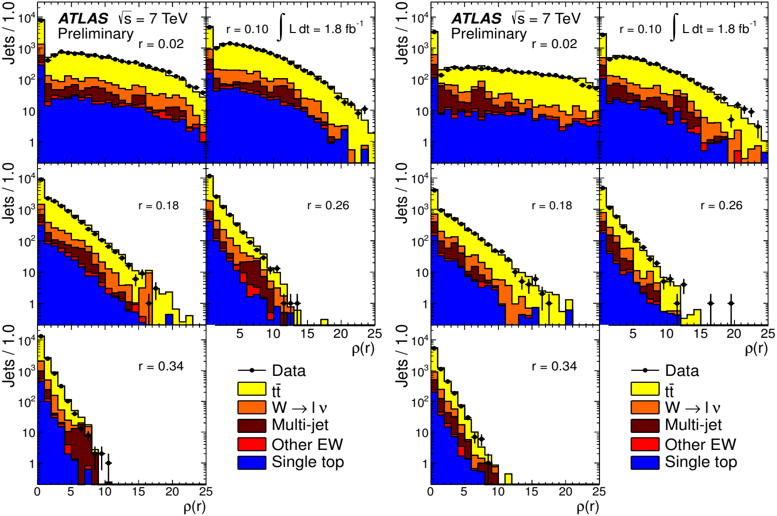

Integrated jet shapes $\Psi(r)$: Comparison

The distributions for $\Psi(r)$ for b (left) and light-jets (right).

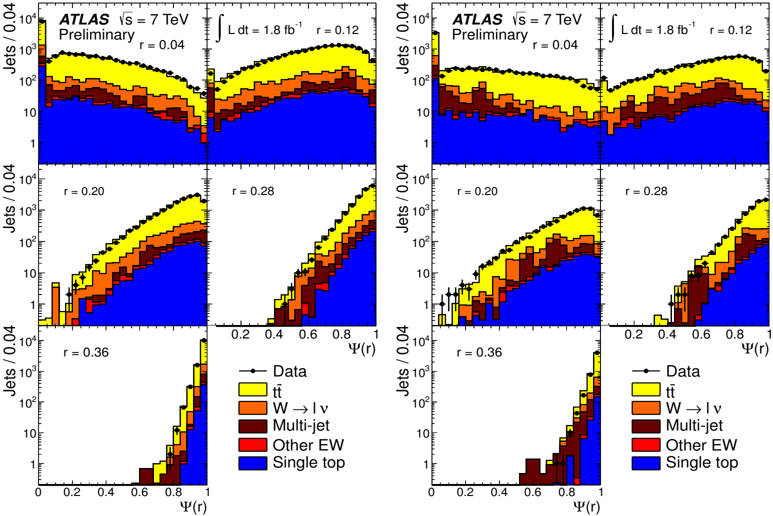

The transverse momentum distributions for *b*-jets in the dileptonic channel (left) and light-jets (right).

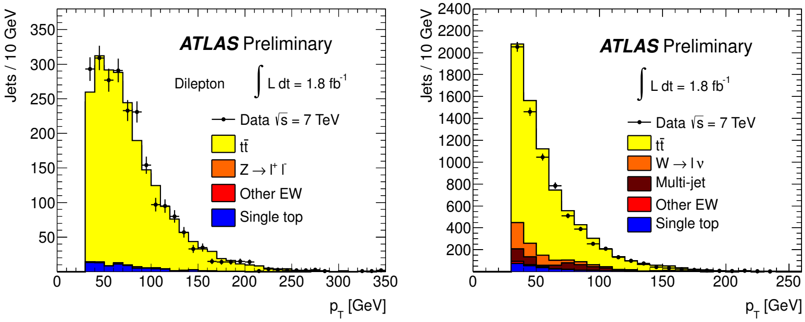

The distributions of ΔR_{jj} for b (left) and light-jets (right).